Manuscript (double-spaced and continuously LINE and PAGE numbered)-for final publication

Click here to view linked References

Minimizing grid energy consumption in wastewater treatment plants: Towards green energy solutions, water sustainability, and cleaner environment

Mohammad Alrbai[1, *], Sameer Al-Dahidi[2], Loiy Al-Ghussain[3, *], Ali Alahmer [4,5], Hassan Hayajneh[6]

[1] Department of Mechanical Engineering, School of Engineering, University of Jordan, Amman 11942, Jordan.

[2] Department of Mechanical and Maintenance Engineering, School of Applied Technical Sciences, German Jordanian University, Amman 11180, Jordan.

[3] Energy Systems and Infrastructure Analysis Division, Argonne National Laboratory, Lemont, IL 60439, USA.

[4] Department of Mechanical Engineering, Tuskegee University, Tuskegee, AL 36088, USA.

[5] Department of Mechanical Engineering, Faculty of Engineering, Tafila Technical University, Tafila 66110, Jordan.

[6] Department of Engineering Technology, College of Technology, Purdue University Northwest, 2200, USA.

*Corresponding authors:

Mohammad Alrbai: Department of Mechanical Engineering, School of Engineering, University of Jordan, Amman 11942, Jordan. m.alrbai@ju.edu.jo.

Loiy Al-Ghussain: Energy Systems and Infrastructure Analysis Division, Argonne National Laboratory, Lemont, IL 60439, USA. Tel. +1 (859) 684-8442. Email: lalghussain@anl.gov.

Abstract:

Wastewater treatment plants (WWTPs) consume significant amount of energy to sustain their operation. From this point, the current study aims to enhance the capacity of these facilities to meet

their energy needs by integrating renewable energy sources. The study focused on the investigation of two primary solar energy systems in As Samra WWTP in Jordan. The first system combines parabolic trough collectors (PTCs) with thermal energy storage (TES). This system primarily serves to fulfil the thermal energy demands of the plant by reducing the demands from boiler units, which allows more biogas for electricity generation. The second system is a photovoltaic (PV) system with Lithium-Ion batteries, which directly produces electricity that will be used to cover part of the electrical energy demands of plant. To assess the optimal configuration, two distinct scenarios have been formulated. The first scenario focuses on maximizing the net present value (NPV) and minimizing the levelized cost of electricity (LCOE). The second scenario is centred on minimizing the levelized cost of heat (LCOH). The findings indicate that both scenarios succeeded in reducing the reliance on the grid to a value that reach 1%. Moreover, they both biogas in energy production from 88% to approximately 65% through the integration of the PV system. In terms of thermal demand, SC#2 reduced the reliance on biogas boiler units from 100% to 25%, while SC#3 achieved an even more impressive reduction to just 8%. The best LCOE value was attained in SC#2, at 0.0895 USD/kWh, with an NPV of 10.54 million USD. Conversely, SC# 3 yielded an LCOH value of 0.0432 USD/kWh_{th} compared to 0.0534 USD/kWh_{th} USD for SC#2. Despite their relatively high capital and operating costs, SC#2 and SC#3 managed to substantially decrease the annual electricity expenditure from approximately 2 million USD to 86,000 USD and 0 USD, respectively.

Keywords: Waste Management; Solar Energy; Sustainability; Economic Analysis; Photovoltaic; Concentrated Solar Power.

1. Introduction

Located in the Middle East, Jordan faces a multitude of challenges related to energy, water, and environmental sustainability. This arid region must prioritize securing both water resources and energy reserves. The issue is particularly pronounced when it comes to wastewater treatment, where maintaining a delicate balance between resource management and environmental stewardship is crucial. Jordanian WWTPs currently face a dual energy challenge. Firstly, they must manage the high energy demands associated with treating wastewater to meet stringent safety standards for disposal and reuse. Additionally, the country's energy situation is marked by scarcity and reliance on imported sources. With over 95% of its energy being imported, Jordan is susceptible to fluctuations in global energy markets and regional geopolitical dynamics, which can impact its energy supply chain (Schuetze & Hussein, 2023).

WWTPs are a paramount process for safeguarding the health and well-being of communities. It serves a dual purpose, not only protecting the environment by eliminating contaminants from wastewater before it is discharged but also playing a pivotal role in conserving water resources and preventing the dissemination of waterborne diseases (Obaideen et al., 2022). However, traditional methods of wastewater treatment consume substantial amounts of energy, contributing to greenhouse gas emissions and escalating operational expenses (Myszograj et al., 2021), (Płuciennik-Koropczuk et al., 2022). In order to tackle these challenges head-on, optimizing energy sustainability in wastewater treatment plants becomes imperative. Prior research endeavors have explored various strategies aimed at enhancing energy efficiency, integrating renewable energy sources, and fostering sustainable practices within wastewater treatment plant (WWTP) operations.

Regarding energy efficiency and minimizing carbon emissions, it has been observed that a substantial amount of energy consumption is associated with wastewater treatment plants. Various studies have highlighted the importance of optimizing energy usage in WWTP facilities (Myszograj et al., 2021) (Maktabifard et al., 2018) (Capodaglio & Olsson, 2020) (Xi et al., 2021). For example, research conducted at the Gubin WWTP in Poland identified that traditional activated sludge-based plants typically require between 0.30 and 1.2 kWh/m^3 of energy (Myszograj et al., 2021). To address this issue, implementing energy-efficient strategies such as operational enhancements and innovative technologies can help reduce overall energy consumption levels. In Chile, Maziotis et al (Maziotis et al., 2023) conducted an energy efficiency study using the tree approach. The results revealed significant energy inefficiency across Chilean WWTPs, with a mean energy efficiency of 0.287, indicating a potential 71.3% reduction in energy usage needed to treat equivalent wastewater volumes. On the other hand, Zhu and Chen (Zhu et al., 2024) showed in a similar study that the typical scarcity-based energy efficiency level of WWTPs in China was found to be low. The study facilitates the formulation of optimal efficiency strategies for WWTPs across various provinces, taking into account potential energy scarcity risks stemming from trading activities.

The integration of biogas and renewable energy technologies in WWTPs has emerged as a promising solution to optimize energy sustainability and address these challenges. Biogas, which is produced through the anaerobic digestion of organic waste, can be harnessed as a source of renewable energy (Kiselev et al., 2024). One potential approach to increase biogas production and energy recovery in wastewater treatment plants is through the co-digestion of organic waste with sludge. This method, discussed in (Mattioli et al., 2017), shows promising results and can significantly enhance biogas yields. Specifically, co-substrates like poultry waste have been found to be highly effective (Masłoń et al., 2020). Furthermore, membrane processes such as membrane distillation and reverse osmosis,

explored in (Zahmatkesh et al., 2022), offer opportunities to improve energy efficiency in WWTPs, which in return reduces the carbon footprint of the plant.

The incorporation of renewable energy sources is crucial for enhancing the sustainability of wastewater treatment plants. Some main wastewater treatment processes, that include the degradation of organic pollutants present in wastewater, involve the activation of a catalyst by light to accelerate chemical reactions in a mechanism known as photocatalysis (Dutta et al., 2024). By harnessing solar energy through photocatalysis, WWTPs can enhance the removal of antibiotics and other contaminants (Patial et al., 2024) (Malhotra et al., 2023), improve water quality (Patial et al., 2023), and reduce reliance on conventional treatment methods (Khan et al., 2023), contributing to overall sustainability and environmental protection efforts.

Renewable energy role in WWTPs is presented also in plentiful studies that investigated the integration of different systems, such as solar photovoltaics (PV) (Guo et al., 2024), biomass gasifiers (Tavakoli et al., 2024), wind turbines, and geothermal energy, into WWTP operations (Zakariazadeh et al., 2024) . Notably, the utilization of combined heat and power (CHP) systems that utilize digester gas or biogas has been emphasized in prior research papers (Mattioli et al., 2017) (Nourin et al., 2020) (Jacob et al., 2020).

According to recent research (Bey et al., 2021), grid-connected PV systems have the potential to fulfill a significant portion of electricity demand for wastewater treatment plants and may even generate surplus power that can be fed back into the grid. To maximize economic viability, hybrid systems that combine multiple renewable energy sources with efficient energy utilization are being considered as favorable options (Buller et al., 2022). It is important to evaluate the economic viability of integrating renewable energy sources with WWTPs. Several studies (Brachi et al., 2022) (Santos et al., 2016) (Đurđević et al., 2019) (Płuciennik-Koropczuk et al., 2022) provide methods for assessing the

feasibility of biogas generation, solar energy, and cogeneration projects. Factors such as population size, energy demand, and government policies influence the potential success of these initiatives (Santos et al., 2016). Furthermore, these projects offer significant benefits in terms of cost reduction and emissions reduction. A case study conducted at Gubin-Guben sewage treatment plant demonstrated these advantages (Sadecka et al., 2013). In another study by Tomczyk et al (Tomczyk et al., 2023), they investigated the hydroelectric capacity of wastewater treatment plants by utilizing the kinetic and/or potential energy from treated wastewater to generate electricity.

The positive environmental impacts of adopting renewable energy sources in WWTPs are clearly evident. Several studies like (Xi et al., 2021) (Đurđević et al., 2019) (Gandiglio et al., 2017) have discussed the significant reduction in greenhouse gas emissions achieved through the utilization of biogas and other energy-efficient strategies. Additionally, the co-digestion of organic waste and sewage sludge (Masłoń et al., 2020) has proven to be a highly effective method for reducing emissions compared to traditional disposal methods. For example, the study done by Aghabalaei et al (Aghabalaei et al., 2023) focused on the greenhouse gas (GHG) emissions and energy WWTPs, emphasizing the importance of reducing both. Initially, the emissions and energy usage of the Mashhad WWTP are compared with energy self-sufficient WWTPs. Four scenarios are then developed, with a focus on transitioning from aerobic to anaerobic digestion. Results show that the WWTP's energy consumption and GHG emissions exceed acceptable levels. By adopting anaerobic digestion and CHP, energy consumption and GHG emissions are significantly reduced by approximately 70% and 53%, respectively. In a recent study by Mannina et al (Mannina et al., 2024), they compares two WWTP configurations: conventional activated sludge (CAS) and oxic-settling-anaerobic process with intermittent aeration (OSA-IA). OSA-IA shows a shift towards sludge

reduction metabolism and lower indirect emissions. Despite slightly lower carbon footprint, both configurations offer valuable insights for optimizing WWTPs for environmental sustainability.

Continued efforts are being made to enhance energy efficiency in WWTPs and incorporate renewable energy sources (Garcia et al., 2024). However, there are still a number of obstacles that must be overcome, such as the complexity of the systems, varying sizes of plants, and the requirement for customized solutions (Gandiglio et al., 2017) (Ali et al., 2020). It is recommended that future studies concentrate on reducing emissions even further, advancing more efficient technologies for energy recovery, and increasing the implementation of renewable energy in wastewater treatment plants (Zahmatkesh et al., 2022) (Chen & Chen, 2013) (Zhang et al., 2024).

In this study As Samra WWTP is examined as a case study to explore ways of improving energy sustainability in WWTPs in Jordan, the main goal is to address the challenges related to energy and water in Jordan while promoting long-term sustainability and resilience. By integrating biogas and other renewable energy systems like PV and PTC in WWTPs, this can optimize energy efficiency and ensure the security of both water resources and energy supply for a sustainable future. To assess the proposed system, an analysis of three key scenarios has been conducted. The first scenario represents the baseline, where no PV or PTC system is in place. In this setting, energy production relies solely on biogas generators, with any remaining energy demands covered by the grid. The second scenario, which optimizes for the maximum NPV and LCOE, incorporates both PV and PTC systems. This approach focuses on meeting electrical energy demands at the lowest possible cost. The third scenario aims at minimizing the LCOH. Here, the system configuration emphasizes satisfying thermal demands by scaling up the PTC and TES systems. The core objective behind examining these scenarios is to pinpoint the optimal approach that effectively eradicates or at least significantly reduces the energy deficit in the plant's operations. As previously discussed, the As Samra water treatment plant currently

generates about 88% of its energy requirements from biogas. This means the facility bears a considerable expense covering the remaining 12%. Hence, exploring renewable energy sources like solar power emerges as an attractive solution to bridge this energy production gap.

2. Materials and Methods

2.1 Study Area: Al Samra WWTP in Jordan

Al Samra Waste Water Treatment Plant, as depicted in Figure 1, is positioned 45 kilometres to the northeast of Amman, within the Hashmeyah / Zarqa governance area. Its geographical coordinates are approximately 32° 14'43.71" north latitude and 36° 10'04.14" east longitude. It is operated by the Samra O&M company under a BOT (Built Operate Transfer) contract that spans 30 years, commencing in 2006 and concluding in 2037. The development of the Samra Project unfolded through two primary phases of expansion. The first phase was initiated in 2007, and the second phase was introduced in 2015.

Figure 1: Satellite view for the location of Al Samra WWTP.

The operation of Al Samra WWTP starts by receiving the coming waste water from Ain Ghazal pre-treatment facility. The inlet raw water flows through a 1500 mm diameter pipe into two Pelton turbines

within the inlet structure, where it is utilized to generate electrical power. The elevation difference between Ain Ghazal and As-Samara WWTP is approximately 78 meters. Subsequently, the treated water combines with incoming wastewater from Zarqa and Hashimiyya stations and is directed into two grits and sulfide removal tanks, each of which is subdivided into multiple chambers. The effluent from these tanks then enters eleven secondary clarifiers, each with a diameter of 54 meters, where suspended solids are separated. A portion of the settled sludge is thickened in flotation units, while the remainder is recycled back into the aeration tanks. The clarified effluent from the secondary settling tanks proceeds to three plug chlorine contact basins, each with a volume of 3500 m^3, where it undergoes approximately 35 minutes of contact with chlorine to achieve final disinfection, meeting Jordanian standards. The effluent is then discharged into three Francis hydraulic turbines, which can produce up to 1300 Kw of power, before being directed to the King Talal Reservoir.

On the other hand, primary sludge from the primary settling tanks undergoes thickening in six enclosed circular thickeners, while biological sludge is thickened within three enclosed dissolved air flotation units. These two streams are blended in a covered reservoir before being transferred to four anaerobic digesters, each boasting a capacity of 15000 m^3. The sludge resides in these digesters for a duration of three weeks, maintained at a temperature of 35°C, and undergoes thorough mixing using recycled compressed biogas. The reheating of the recycled sludge is accomplished by utilizing hot water from the boiler unit, which passes through a shell and tube heat exchanger. After digestion process, the sludge is directed to a digested sludge storage tank and subsequently pumped into 25 solar evaporation basins, where it is dried to achieve a dry solids content of approximately 30%. Lime which may be used if necessary for sludge stabilization. The biogas generated in the digesters is stored in four gas holders, each with a capacity of 5000 m^3, and undergoes H_2S removal before being utilized to power ten biogas engine generator in addition to the boiler unit.

Figure 2 illustrates the biogas generation process, beginning at the sludge thickeners (marked as point 1) and extending to the biogas storage tanks (point 5). Processes unrelated to the current study have been omitted from the figure. Additionally, Figure 2 introduces the new renewable energy systems proposed in this study to address the plant's energy requirements. The study investigates two solar energy systems, comprising both photovoltaic (PV) and parabolic trough collectors (PTCs) systems. The integration of these two systems serves the primary purpose of fulfilling the energy demands of the Al Samra WWTP and reducing its reliance on the grid. Figure 3 displays the total energy consumption at the Al Samra WWTP, along with the energy obtained from the JEPCO (Jordanian Electric Power Company) grid network over the past five years. As depicted in the figure, the plant has averaged around 215 MWh of energy consumption per day. This energy demand is primarily met by the biogas power generators and by the existing hydraulic turbines at the inlet and exit of the plant, accounting for approximately 88% of the total energy requirement. The remaining energy is sourced from the grid, with an average daily consumption of 27 MWh.

To fulfill the energy needs of the plant from the grid, two key modifications are proposed to make use of the available land surrounding the facility. Firstly, the installation of a photovoltaic (PV) system is suggested, which can generate electrical energy to supply part of the plant's facilities energy requirements instead of depending on grid energy. Secondly, the utilization of PTC solar systems is recommended to satisfy the heating requirements of the digester units. According to data provided by the Al Samra WWTP operator, approximately 10% of the total biogas produced is used by the boiler unit. This portion can be entirely or partially utilized by employing a solar thermal system like PTC collectors with thermal energy storage (TES). Such a modification would allow the biogas generators to produce more electrical energy, subsequently reducing the reliance on grid power. In the following sections, the authors explore the modeling of both PV and PTC systems, including an analysis of their

performance within the plant's operation. Furthermore, a Techno-economic study regarding the integration of these two systems is also included.

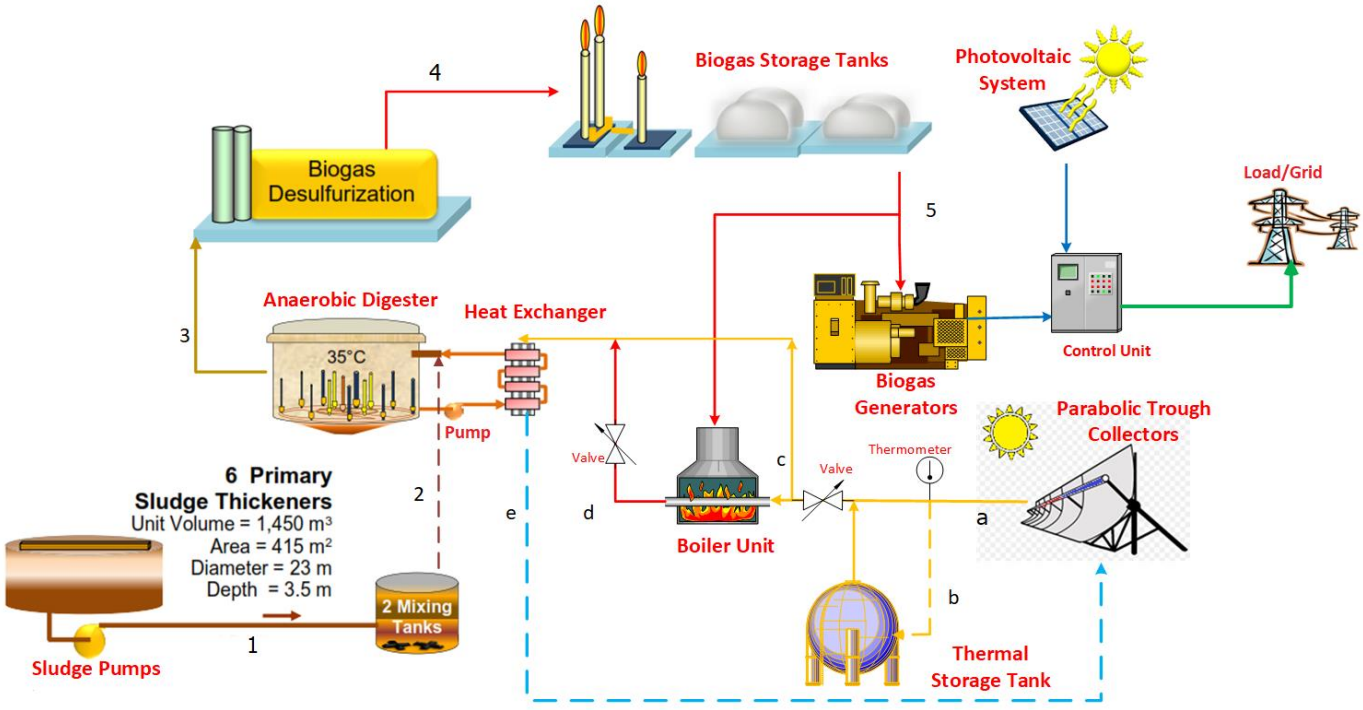

Figure 2: Schematic of Al Samra WWTP biogas production process including the integration of PV & PTC solar systems.

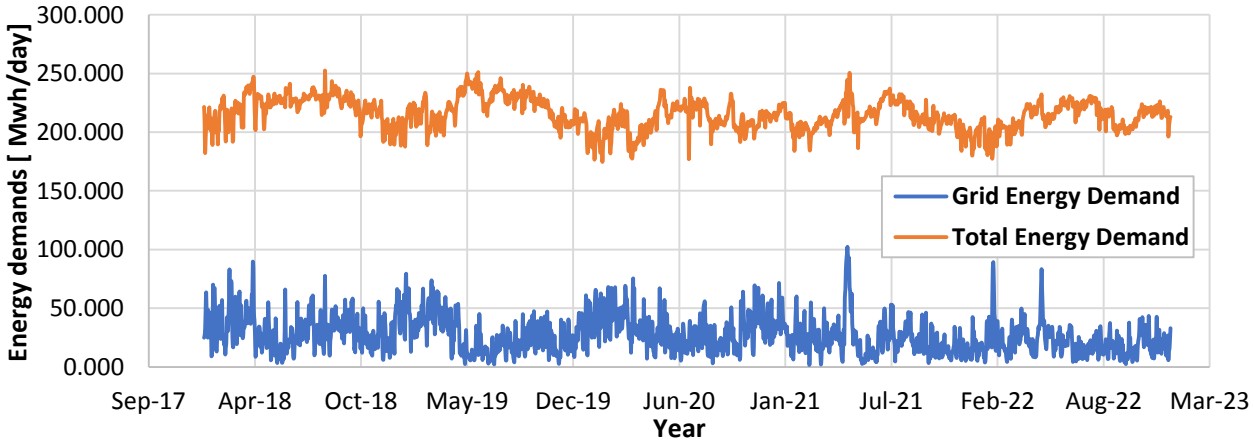

Figure 3: Al Samra WWTP total energy demands and the grid energy demands for the last five years [2018-2022].

2.2 Materials and Mathematical Models

2.2.1. PTC and TES systems

The performance of the PTC model relies upon the establishment of an energy equilibrium between its constituent components, namely, the collector and the heat collector element (HCE). This equilibrium serves as the foundational underpinning for the HCE. It encompasses the integration of direct normal solar irradiance incident upon the collector into the energy balance, as well as the incorporation of optical losses arising from both the collector and the HCE, thermal losses emanating from the HCE, and the accrual of heat within the heat transfer fluid (HTF). All forms of the involved heat energy within the HCE are described in Figure 4. Here, one-dimensional energy balance is used to model LS-2 PTC with Syltherm 800 as the HTF with a mass flow rate of 0.1 kg/s. The technical specifications of the proposed PTC and HCE model are listed in Table 1 where the numbers shown with symbols are defined based on Figure 4.

Table 1: LS-2 Specifications of the investigated PTC system (Al-Ghussain et al., 2022)

PTC component	Property/Dimension	Symbol	Value	Unit
Mirrors	Reflectivity	ρ_{cl}	0.93	-
	Length	L	7.8	m
	Aperture width	W	5	m
	Focal length	f	1.71	m
Glass cover	Material	-	Borosilicate Glass	-
	Thickness	t_{4-5}/t_{6-7}	2.5	mm
	Absorptivity	α_5/α_7	0.02	-

	Transmissivity	τ_5/τ_7	0.935	-
	Emissivity	$\varepsilon_5/\varepsilon_7$	0.86	-
	Thermal conductivity	k_{4-5}/k_{6-7}	1.04	W/m.K
	Inner diameter	$D_{g,i}$	0.115	m
	Outer diameter	$D_{g,o}$	0.12	m
Absorber tube	Material	-	SS 304L	-
	Thickness	t_{2-3}	10	mm
	Absorptivity	α_3	0.96	-
	Emissivity	ε_3	0.14	-
	Thermal conductivity	k_{2-3}	$0.013\,T_{23} + 15.2$	W/m.K
	Inner diameter	$D_{a,i}$	0.066	m
	Outer diameter	$D_{a,o}$	0.07	m

Optical losses can arise from multiple sources, such as imperfections in the collector mirrors, tracking inaccuracies, shading effects, the accumulation of contaminants on the HCE and mirrors, among others. Within this energy balance framework, the effective solar energy, defined as the total incident solar energy minus the optical losses, is subsequently absorbed by the absorber ($\dot{q}'_{5\ \mathrm{SolAbs}}$) specifically its selective coating layer and also by the glass envelope ($\dot{q}'_{3\ \mathrm{SolAbs}}$). A portion of the energy absorbed by the selective coating undergoes thermal transfer via conduction to the absorber ($\dot{q}'_{23\ \mathrm{cond}}$) followed by convection into the HTF ($\dot{q}'_{12\ \mathrm{conv}}$), The residual energy is subsequently transferred back to the glass envelope via convective ($\dot{q}'_{34\ \mathrm{conv}}$)and radiation ($\dot{q}'_{34\mathrm{rad}}$) Additionally, there is an energy loss

through conduction across the support structure of the HCE ($\dot{q}'_{\text{cond,bracket}}$).

The energy transmitted back to the glass envelope is then conducted through it ($\dot{q}'_{45\ \text{cond}}$) where it is ultimately dissipated along with the previously absorbed energy through convective ($\dot{q}'_{56\text{conv}}$) and radiation ($\dot{q}'_{57\text{rad}}$) processes into the surrounding environment. It's worth noting that in the absence of a glass envelope, the energy loss from the absorber occurs directly into the surrounding environment. In the context of this model, it is assumed that all physical properties are uniform throughout the circumference of the HCE, and the depicted flux directions are considered positive.

The conservation of energy at the surfaces of the HCE, assuming glass envelope, is presented through Eq. (1) to Eq. (5):

$$\dot{q}'_{12\ \text{conv}} = \dot{q}'_{23\ \text{cond}} \tag{1}$$

$$\dot{q}'_{3\ \text{SolAbs}} = \dot{q}'_{34\ \text{conv}} + \dot{q}'_{34\text{rad}} + \dot{q}'_{23\ \text{cond}} + \dot{q}'_{\text{cond,bracket}} \tag{2}$$

$$\dot{q}'_{34\ \text{conv}} + \dot{q}'_{34\text{rad}} = \dot{q}'_{45\text{cond}} \tag{3}$$

$$\dot{q}'_{45\ \text{cond}} + \dot{q}'_{5\ \text{SolAbs}} = \dot{q}'_{56\text{conv}} + \dot{q}'_{57\text{rad}} \tag{4}$$

$$\dot{q}'_{\text{HeatLoss}} = \dot{q}'_{56\ \text{conv}} + \dot{q}'_{57\text{rad}} + \dot{q}'_{\text{cond,bracket}} \tag{5}$$

It is noteworthy that the phenomenon of absorption in both opaque (the absorber) and semi-transparent materials (the glass envelope) is inherently a volumetric consideration. However, it is pertinent to acknowledge that most of absorption events occur near the material surface. Furthermore, the absorptance of the glass envelope is relatively modest. Consequently, the approximation of addressing solar absorption as a surface-based problem introduces only a negligible error. In this context, the term "solar absorptance" remains valid and accurate when characterizing this behavior. The terms ($\dot{q}'_{3\ \text{SolAbs}}$) and $\dot{q}'_{5\ \text{SolAbs}}$ represent heat flux components that are employed as simplifications for solar absorption, facilitating the treatment of heat conduction through both the absorber and the glass envelope as linear processes.

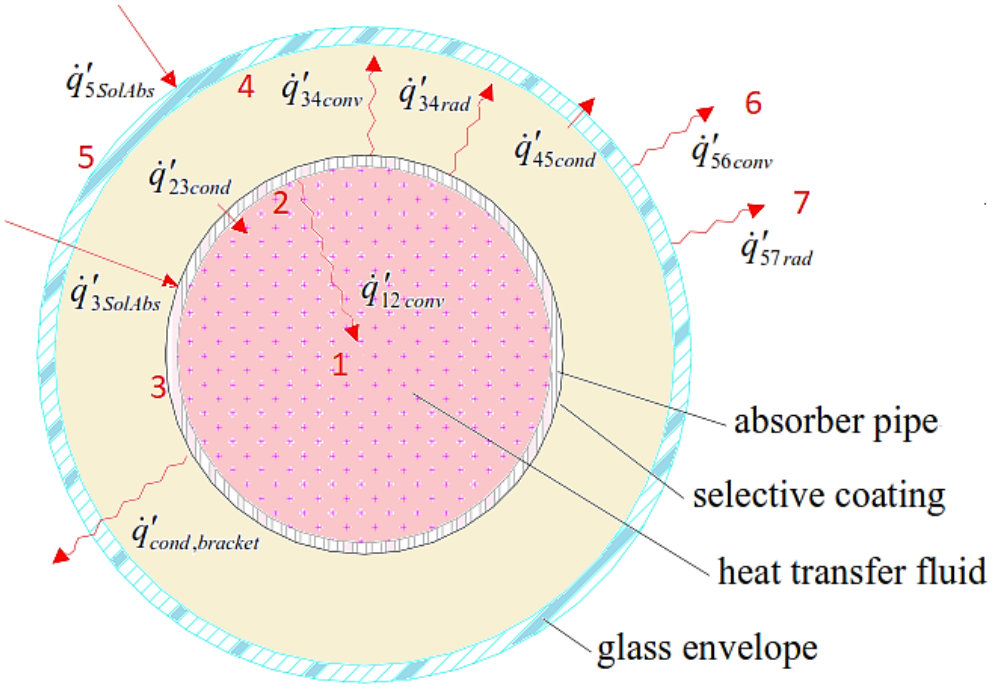

Figure 4: One-dimensional steady-state energy balance for HCE element in PTC system.

2.2.2. PV model

In this section, the method used to calculate the hourly energy generation of the PV station within the proposed system is presented. This method consists of three primary steps, which are illustrated as following:

Step 1: Calculation of the Incident Angle. The incident angle (θ) can be found using the steps presented in (Duffie & Beckman, 2006). The computation goes along the following procedure:

The sun's position in the sky is determined by several factors, including the solar time (ts), the day of the year (d), and the latitude of the geographical location (ϕ). Solar time (t_s) can be e calculated using the formula in Eq. (6):

$$t_s = t_{std} + 4 \times (L_{st} - L_{loc}) + E \quad (6)$$

In Eq (1), t_{std} represents standard time, L_{st} and L_{loc} are the standard and local meridians, respectively, and E accounts for the time equation.

Subsequently, the solar time is transformed into an angular representation to determine the angle of the sun's position, as indicated by Eq. (7):

$$\omega = (t_s - 12) \times 15 \tag{7}$$

Where, ω is the hour angle, i.e., the angular displacement between the sun's surface and the observer's meridian.

To assess the influence of the day of the year on the sun's position in the sky, one can determine the declination angle (δ), which represents the angle between the equatorial plane and the solar radiation beam at solar noon. This can be accomplished using Eq. (8):

$$\delta = 23.45 \times \sin(360 \times \frac{284+n}{365}) \tag{8}$$

In Eq (3), n accounts for the number of days in the year, and the declination angle values vary within the range of -23.45° to +23.45°.

The sun's position is characterized by two angles: i) the zenith angle (θz) and ii) the solar azimuth (γ_s). The zenith angle represents the angle between the line pointing to the sun and the vertical direction. It can be calculated using Eq. (9):

$$cos\ \theta z = cos\ \phi\ cos\ \delta\ cos\ \omega + sin\ \phi\ sin\ \delta \tag{9}$$

297

298 On the other hand, the solar azimuth refers to the compass direction from which sunlight arrives.
299 This can be computed using Eq. (10):

$$\gamma_s = \text{sign}(\omega) \times \left|\cos^{-1}\left(\frac{\cos\theta z \sin\phi - \sin\delta}{\sin\theta z \cos\phi}\right)\right| \quad (10)$$

300 In conclusion, the angle of incidence (θ) signifies the angle formed between the solar radiation
301 beam and the surface of the solar system. It can be determined through Eq. (11):

$$\cos\theta = \cos\theta z \cos\beta + \sin\theta z \sin\beta \cos(\gamma_s - \gamma) \quad (11)$$

302 Here, β, which represents the tilt angle of the solar system, and γ (i.e., the surface azimuth) are key
303 factors in the solar system setup.

304 **Step 2: Estimation of Radiation Incident on Tilted Surface.** The determination of solar radiation
305 received by an tilted surface (I_T) involves the application of the isotropic diffuse model as outlined in
306 (Duffie & Beckman, 2006). More specifically, I_T encompasses three distinct components: i) direct
307 beam radiation (I_b), ii) isotropic diffuse radiation (I_d), and iii) solar radiation that has undergone
308 diffuse reflection from the ground ($I\rho_g$). It should be emphasized that, for the purposes of this study,
309 the consideration of reflected radiation has been omitted.

310 The calculation for I_T is provided by Eq. (12):

$$I_T = I_b R_b + I_d\left(\frac{1 + cos\beta}{2}\right) \quad (12)$$

311 Here R_b denotes the proportion of beam radiation received on the tilted surface in comparison to that
312 received on a horizontal surface at any given moment. It's noteworthy that the hourly data for diffuse
313 and direct solar radiations, as well as ambient temperature, were obtained from the PVGIS

314 software(*EU Science Hub, Non-Interactive Service*, 2023; Huld et al., 2012), based on typical
315 meteorological year (TMY) records.

316 **Step 3: Estimation of Energy Generated by the PV system.** To calculate the energy output generated
317 by the PV system (E_{PV}) for each hour, Eq. (15) is employed. This calculation necessitates the
318 determination of three key factors: the efficiency of the PV module (η_{PV}) (using Eq. (13)), the
319 temperature of the PV cells (T_{PV}) (using Eq. (14)), and the previously calculated solar radiation on the
320 tilted surface (I_T) as described in Eq. (12):

$$\eta_{PV} = \eta_{PV,Ref} \times \left(1 - \beta_{Ref} \times \left(T_{PV} - T_{Ref,STC}\right)\right) \quad (13)$$

$$T_{PV} = T_{amb} + \left(\mathrm{NOCT} - T_{Ref,NOCT}\right) \times \frac{I_T}{I_{Ref}} \quad (14)$$

$$E_{PV} = \eta_{PV} \times I_T \times A_m \times N_m \times PR \quad (15)$$

321 In Eq.(13) through Eq.(15), T_{amb} represents the ambient temperature, A_m corresponds to the module's
322 surface area, N_m stands for the total number of modules in the system, and PR denotes the performance
323 ratio of the PV system, which, for this analysis, is assumed to be 0.85 based on (Al-Ghussain et al.,
324 2018). It's important to note that the calculations are facilitated by the following realistic yet
325 straightforward assumptions: i) uniform cell temperature across all PV modules, ii) a uniform
326 efficiency for all PV modules, and iii) uniform solar radiation received by all solar panels. Technical
327 specifications for the PV module (HiKu7_CS7N-MS) used in this study are detailed in Table 2
328 (CanadianSolar, 2021).

329 **Table 2**: PV module (HiKu7_CS7N-MS) specifications (CanadianSolar, 2021).

Parameter	Value	Description
Module rater capacity (W)	670	PV module rater capacity

$\eta_{PV,Ref}$ (%)	21.6	Reference PV efficiency
β_{Ref} (1/°C)	-0.0034	PV power loss coefficient
$T_{Ref,STC}$ (°C)	25	Standard cell temperature
NOCT (°C)	41	The temperature of the cell under normal operating conditions
$T_{Ref,NOCT}$ (°C)	20	The reference temperature of the cell under nominal operating conditions
I_{Ref} (W/m^2)	800	The reference solar radiation incident on the PV module
A_m (m^2)	3.11	Area of the PV module

2.2.3 Biogas Energy Production

As mentioned before, the plant is currently meeting around 88% of its energy needs through two existing systems. The first and the main one is the gas power generation unit system. This system consists of 10 biogas power generation units (Caterpillar Model G3516 ZBA) with a power output of 10.7 MW. The plant also generates electrical energy through existing hydraulic turbines at the inlet and exit of the plant. Two Pelton turbines are installed at the inlet of the plant and receive wastewater from the Ain Ghazal area with a net head of 80 m, producing a net power output of 1.76 MW. However, at the exit of the plant, there are 3 Francis turbines that receive the exit flow from a head of 42.8 m, resulting in a net power generation output of 2.13 MW.

All the required data for the current existing systems have been collected and managed by the plant operator. Therefore, this eliminates the need for modeling the power generation process for the

biogas power generation units and the hydraulic turbine unit. Instead, the authors refer to the measured data to perform the remaining calculations for the study, as this data represents the real and actual state of power within the plant. It is worth noting that the data for the biogas generation units and the hydraulic turbines were obtained from the plant operator over the last 5 years, and a sample of this data is presented in Figure 3.

2.2.4 Energy Dispatch Strategy

To increase the utilization of solar energy, we assess the use of closed-loop thermal energy storage (TES) with the PTC whereas we use lithium-ion batteries with the PV system. The TES uses molten salt as HTF where we assume constant thermal losses of about 5% daily (Epp, 2018). On the other hand, for modeling the battery system, we assume 95% round trip efficiency and 85% depth of discharge.

Logic-based energy dispatch strategy was adopted in this study for covering both thermal and electrical demands with the following roles,

- For the thermal demand:
    - The algorithm checks if the thermal energy from the PTC is enough to cover the thermal demand.
    - If the PTC energy is not enough, the algorithm uses the TES to cover the deficit.
    - If the TES does not have enough energy to cover the deficit, biogas boiler is used to cover the remaining deficit.
    - Curtailment of PTC is used in times of excess thermal energy.
- For the electrical demand:
    - The algorithm checks if the electrical energy from the PV is enough to cover the

electrical demand.

- If the PV energy is not enough, the algorithm uses the battery to cover the deficit.
- If the battery does not have enough energy to cover the deficit, the algorithm checks if the electricity from the hydro system is enough to cover the deficit.
- If the hydroelectricity is not enough, the algorithm checks if there is any remaining biogas (after covering the deficit in thermal demand if any) that can be used in the biogas generators to cover the deficit.
- If the electrical energy from the biogas generators is not enough, the algorithm uses the grid to cover the electrical deficit at tariff of 0.225 USD/kWh.
- Due to the current regulations in Jordan as well as the agreement between the WWTP and the grid utility, we assume that only the electrical energy from biogas/hydro is sold to grid at an assumed Power Purchase (PP) tariff of 0.1125 USD/kWh which is half the average tariff in Jordan. Whereas, excess energy from PV is used as a credit for the user to offset the grid bill.

2.2.5 Techno-Economic Feasibility of the Proposed System

It is crucial to evaluate the economic viability of renewable energy sources (RES) in conjunction with their technical feasibility. This study incorporates the assessment of RES from an economic perspective, considering three key parameters: Levelized Cost of Electricity (LCOE), Levelized Cost of Heat (LCOH), and Net Present Value (NPV), each defined as in Eqs.(16-18) (Al-Ghussain et al., 2022):

$$LCOE = \frac{C_{PV} + C_B + \sum_{y=1}^{LT} \frac{M_{PV} + F_{el}}{(1+dr)^y}}{\sum_{y=1}^{LT} \frac{\sum_{t=1}^{8760} D_{el}^t + D_{ex,biogas/hydro}}{(1+dr)^y}} \quad (16)$$

$$LCOH = \frac{C_{PTC} + C_{TES} + \sum_{y=1}^{LT} \frac{M_{PTC} + F_{th}}{(1+dr)^y}}{\sum_{y=1}^{LT} \frac{\sum_{t=1}^{8760} D_{th}^t}{(1+dr)^y}} \quad (17)$$

$$NPV = \sum_{y=1}^{LT} \frac{R_y}{(1+dr)^y} - C_{PV} + C_B + C_{PTC} + C_{TES} \quad (18)$$

Where, C denotes the initial capital and M is the annual maintenance and operation costs where the subscripts PV, B, PTC and TES refer to PV, battery, parabolic trough collector and TES systems respectively. dr is the annul discount rate which assumed to be 8.5%, F is annual biogas fuel cost used to cover the electrical demand (with el subscript) and thermal demand (with th subscript) assuming 0.388 USD/m^3 biogas cost based on the information provided by the WWTP operator, LT is the lifespan of the system and R_y is the annual revenues. D_{el}^t and D_{th}^t are the electrical and thermal demands, respectively whereas $D_{ex,biogas/hydro}$ is the excess energy sold to grid from the biogas and hydro. The economic parameters adopted in this work are shown in Table 3.

Table 3: The projected capital and maintenance expenses for RES and energy storage systems (ESSs) in the year 2030, along with their expected operational lifespans.

System	Capital Cost	Ref.	Annual O&M cost	Ref.	Lifespan
PV system	773.68 [USD/kW$_e$]	(*2030 Solar Cost*	5 [USD/kW$_e$]	(SAFT, 2013),	25 years

		Targets, n.d.)		(Jaber et al., 2004)
PTC system	222.6 [USD/kW_{th}]	(Boretti & Castelletto, 2021)	21 [USD/kW_{th}]	(Boretti & Castelletto, 2021)
Lithium-Ion battery system	150 [USD/kWh_e]	(Cole & Frazier, 2019)	-	
TES	10 [USD/kWh_{th}]	(Parrado et al., 2016)	-	

To achieve the optimal solution in this study, a nonlinear solving algorithm is employed. This algorithm takes into account various variables governing the hybrid system, with nonlinear relationships between the capacities of the system's components. The Generalized Reduced Gradient (GRG) algorithm is utilized to assess the optimal capacities of these components. This algorithm is capable of handling nonlinear inequality constraints. Throughout the search process, a careful balance is maintained, ensuring that dynamic requirements remain accurate even with minor adjustments. In cases where some dynamic requirements are not fully met due to the nonlinearity of limitation functions, the Newton-Raphson technique is implemented to bring the system back to compliance with the specified requirements (Al-Ghussain et al., 2021). The modeling and optimization of RESs are carried out using Microsoft Excel and subsequently validated in (SAFT, 2013).

406 The central aim of the optimization process is to attain the minimum LCOE in SC#2, a crucial metric
407 for assessing the long-term cost-efficiency of a power generation system SC#3. Within this
408 optimization framework, the primary focus is on the capacity levels of the PV,
409 PTC, battery and TES, as these variables significantly influence the system's performance and
410 economic viability.

411 ## 3. Results and Discussion

412 As previously highlighted, a portion of the biogas produced on-site is consumed in the boiler to
413 maintain a specific temperature that ensures the continued functioning of bacteria during biogas
414 production. Two primary systems have been introduced to address this challenge. The first is the PTC
415 system, which harnesses solar energy to heat a closed-loop HTF circuit, facilitating efficient heat
416 exchange with the sludge in the digesters. The second is the TES tank, which stores preheated molten
417 salt at the required temperature, ready for use when the PTC system alone cannot meet the thermal
418 demand. In cases where both the PTC system and the energy storage tank fall short of meeting the
419 digester's energy requirements, a conventional boiler steps in, utilizing biogas to cover the remainder.
420 This approach not only ensures continued biogas production but also yields surplus biogas for use in
421 electrical generators, further increasing electrical energy output.

422 The second facet of the renewable energy strategy is the PV system, responsible for direct electrical
423 energy generation from sunlight. It's worth noting that employing the PV system in isolation is
424 suboptimal due to its inherent energy production variability, in contrast to biogas generators, which
425 maintain a relatively stable power output. Consequently, the study employs both PTC and TES
426 systems to enhance electrical energy production from the biogas generators, thus providing a more
427 reliable and cost-effective energy solution.

To offer a comprehensive overview of the present circumstances at the As Samra WWTp, Figure 5 presents a graphical representation of key parameters. This figure illustrates the daily thermal energy demands of the digesters throughout the year, the daily deficits in electrical energy supply within the facility, and the associated losses in electrical energy production attributable to the consumption of biogas in the boiler unit. Evidently, Figure 5 demonstrates that the average daily deficit in electrical energy demand fluctuates within a range of 8.5 to 9.5 MWh over the course of the year. However, upon a strategic evaluation of the system, taking into account the conservation of thermal energy previously expended in distant operations and its redirection for electrical energy production, it becomes apparent that the potential for daily electrical energy generation amounts to approximately 1.8 MWh.

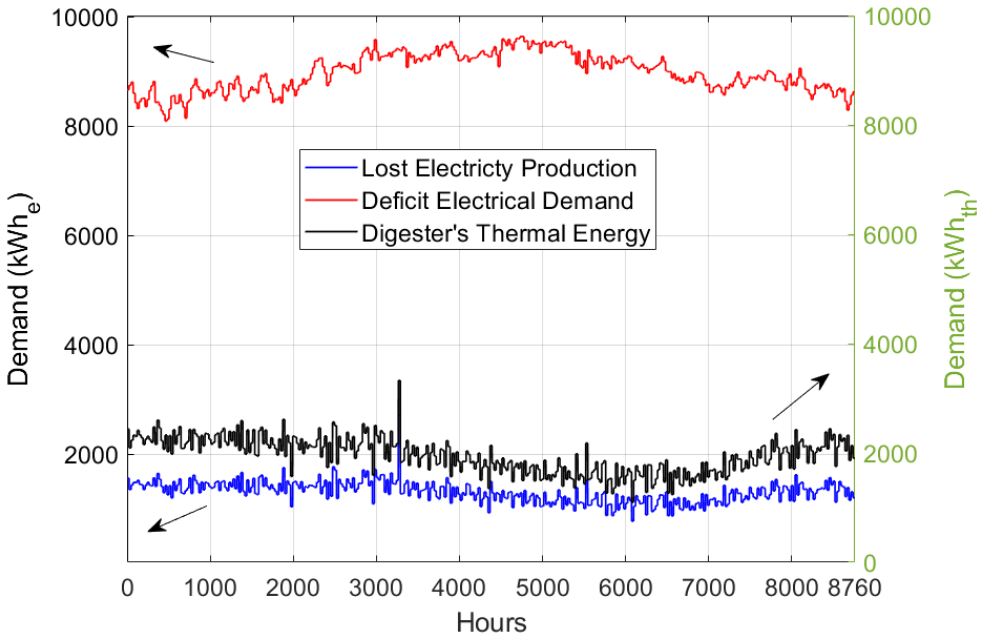

Figure 5: Deficit in electrical energy in As Samra WWTP and the associated lost electrical energy caused by the digester thermal demands.

Table 4 provides a comparative analysis of the three main scenarios with respect to their LCOE, LCOH, and NPV values. In SC#1, the electrical demand is met by a combination of grid-supplied energy and biogas generators which is the current situation at the WWTP. This is reflected in the LCOE and LCOH values, which are 0.1407 USD/kWh and 0.1441 USD/kWh_{th}, respectively. The NPV value for this scenario is -22.35 USD, indicating a lack of profitability. Transitioning to SC#2 involves the introduction of a 19 MW PV system, a 7 MW PTC system, and a 25 MWh_{th} TES system. This transition results in a reduction of electrical energy produced by biogas from 88% to 65%. In this setup, 32% of the plant's electrical energy demand is satisfied by the PV system, with only 3% relying on grid supply. Regarding thermal demand, 75% of the digester's thermal needs are met by the PTC system, while 25% are addressed by the biogas boiler. This scenario succeeds in reducing the LCOE to 0.0895 USD/kWh and the LCOH to 0.0534 USD/kWh_{th}. The NPV value for this scenario is 10.54 million USD, indicating a profitable outcome.

In the context of SC#3, the emphasis is on achieving a minimum LCOH value. To attain this objective, larger PV and PTC systems are required to reduce the dependence on biogas energy. In SC#3, the PV system accounts for 38% of the electrical power production, with biogas responsible for 67%, and the grid covers the remaining 1%. In terms of thermal energy demand, this scenario successfully covers 92% using the PTC and TES systems, while the boiler fulfils the remaining 8%. This shift is reflected in the availability of biogas for electrical generators, resulting in a 2% increase compared to SC#2. Additionally, this scenario boasts lower LCOE and LCOH values than the baseline scenario, with an NPV value of 9.45 million USD. In light of these findings, SC#2 emerges as the most favourable option, based on its superior NPV and LCOE values. Notably, in SC#2 and SC#3 the use of battery is not feasible due to it is high capital cost where the algorithm prefers to use the grid as storage system especially with the current net metering regulations in Jordan.

464 **Table 4:** Optimization results for the three scenarios based on electrical and thermal energy shares.

465

Specification		Base	Max NPV& min LCOE	Min LCOH
PV Plant Capacity (kW)		0	19413.86	36828.17
PTC Capacity (kW_{th})		0	6678.77	11123.59
TES Capacity (kWh_{th})		0	25456.54	69680.70
TES Duration (hours)		0	7.60	20.80
Battery Capacity (kWh)		0	0	0
Battery Duration (hours)		0	0	0
Electric	Ratio met by PV	0%	32%	38%
	Ratio met by biogas	88%	65%	67%
	Ratio met by grid	12%	3%	1%
Thermal	Ratio met by PTC	0%	75%	92%
	Ratio met by biogas	100%	25%	8%
Excess sold to gird	LCOE (USD/kWh)	0.1407	0.0895	0.0954
	LCOH (USD/kWh_{th})	0.1441	0.0534	0.0432
	NPV (MUSD)	-22.35	10.54	9.45
	SC#	**1**	**2**	**3**

466 Figure 6 illustrates the daily coverage of thermal demand in the digesters for each of the proposed
467 scenarios. In SC#1, as depicted in the figure, the thermal demand is entirely satisfied by the boiler,
468 achieved through the combustion of biogas. Turning attention to SC#2, the thermal demand is
469 primarily met by the PTC system, with a supplementary contribution from thermal energy storage.
470 Consequently, the boiler still plays a significant role in this scenario, especially during colder and

cloudier periods throughout the year. This observation aligns with the strategy of SC#2, which prioritizes maximizing the NPV value.

In SC# 3, Figure 6 reveals that the PTC and thermal energy storage systems are capable of almost completely meeting the total thermal demand of the digesters, with only occasional shortfalls during certain periods of the year. This, however, necessitates larger PTC and TES systems, resulting in a reduction in NPV while minimizing the LCOH value. The results point to the fact that in SC# 3, the heat supply from the energy storage tank should be relatively higher compared to the other scenarios. Furthermore, the boiler units are required both at the beginning and end of the year. This nuanced understanding of thermal demand coverage and the interplay of different system components provides valuable insights into the design and operation of the proposed scenarios.

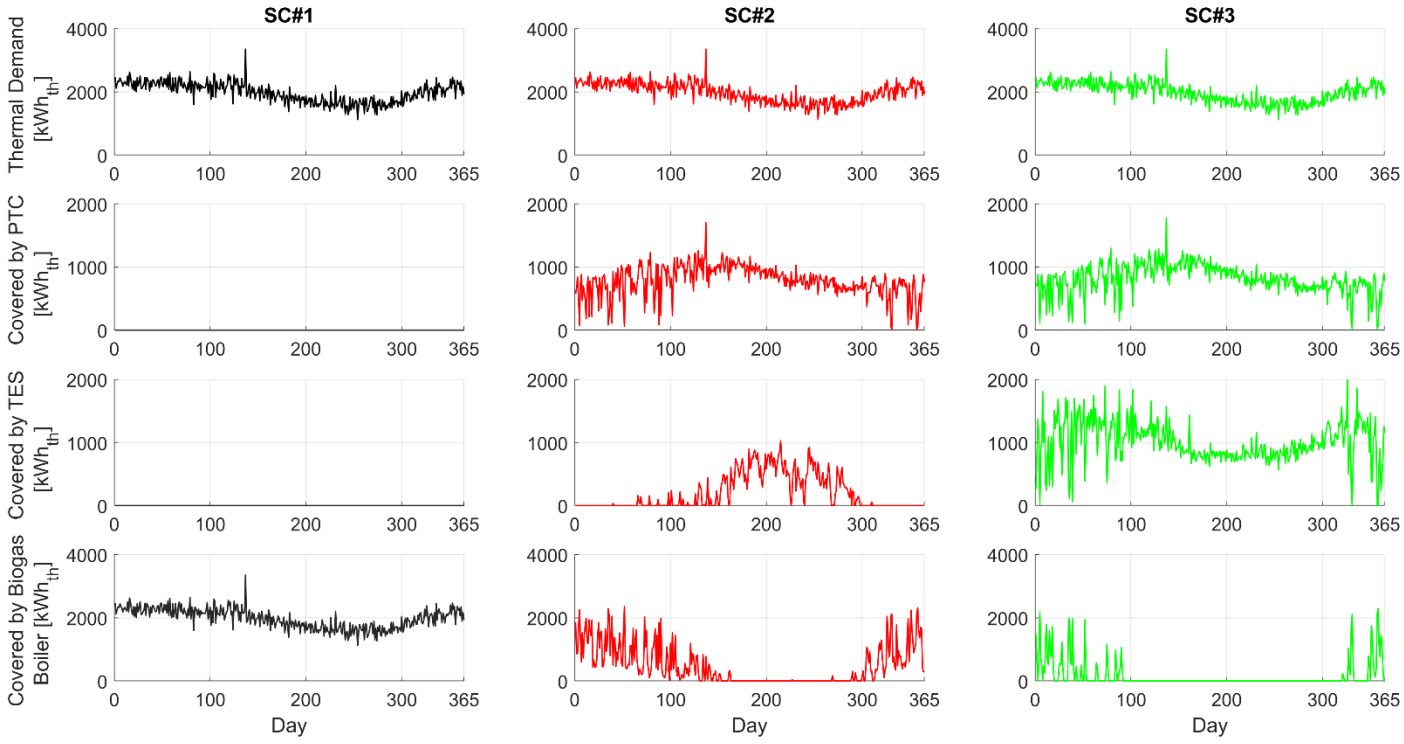

Figure 6: Thermal demand covering throughout the year for the three different scenarios.

To provide a clearer understanding, the performance of each scenario on two specific days, one in summer (1st of June) and the other in winter (1st of December), is detailed in Figure 7. This comparative analysis illuminates the operational distinctions between seasons and underscores the pivotal role played by the PTC and TES systems in scenarios 2 and 3. On June 1st, SC# 2 effectively fulfils the thermal demand, primarily relying on the PTC system. However, in the early morning, the biogas boiler supplements the thermal needs, with the TES system contributing towards the latter part of the day. This strategic coordination enables SC# 2 to optimize energy utilization. Conversely, SC# 3, characterized by larger PTC and TES systems, manages to seamlessly cover the thermal demand throughout the day, without requiring the assistance of the biogas boiler. As previously noted, this approach increases the surplus biogas available for electrical generators, resulting in additional electrical power generation.

Transitioning to December 1st, Figure 8 indicates that the reduced availability of solar hours poses a challenge for the PTC system, leading to an increased reliance on the TES system, especially in the early hours. During this period, the biogas boiler plays a more substantial role in meeting thermal demand. In contrast, SC#3's configuration proves advantageous. The increase in the PTC and TES systems capacities help in covering the thermal demand despite the drop in the solar resources, with the TES system efficiently covering the thermal requirements at the beginning and end of the day.

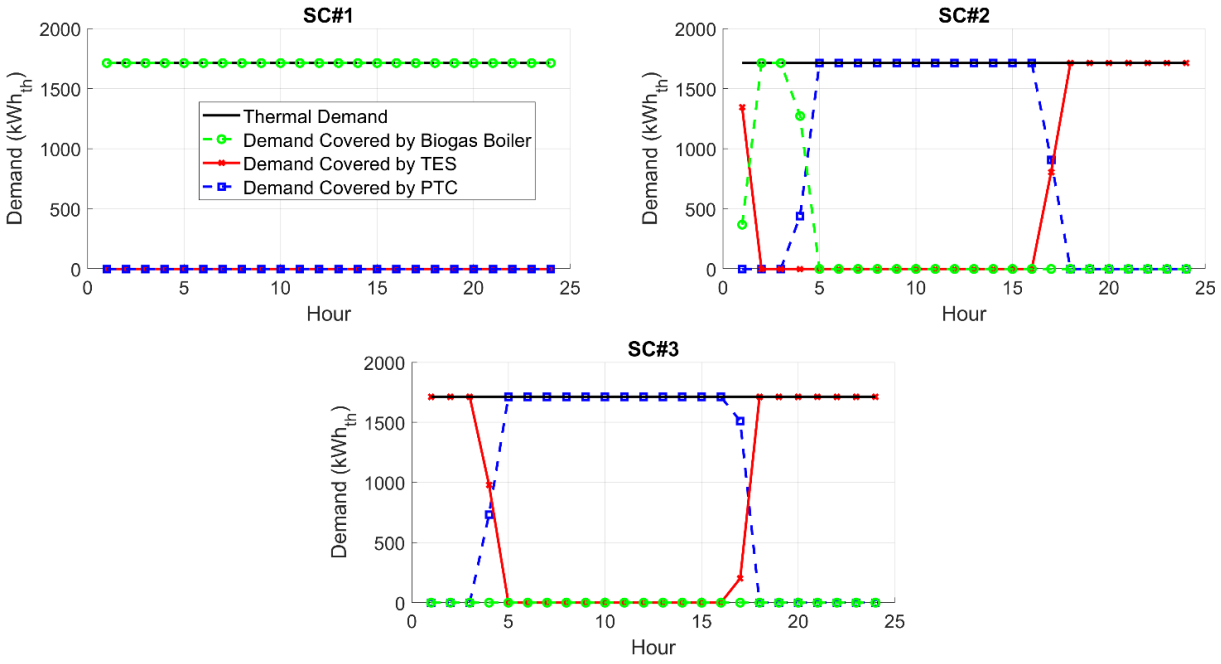

501

502 **Figure 7**: Thermal demand covered by biogas boiler, PTC and TES for June 1st.

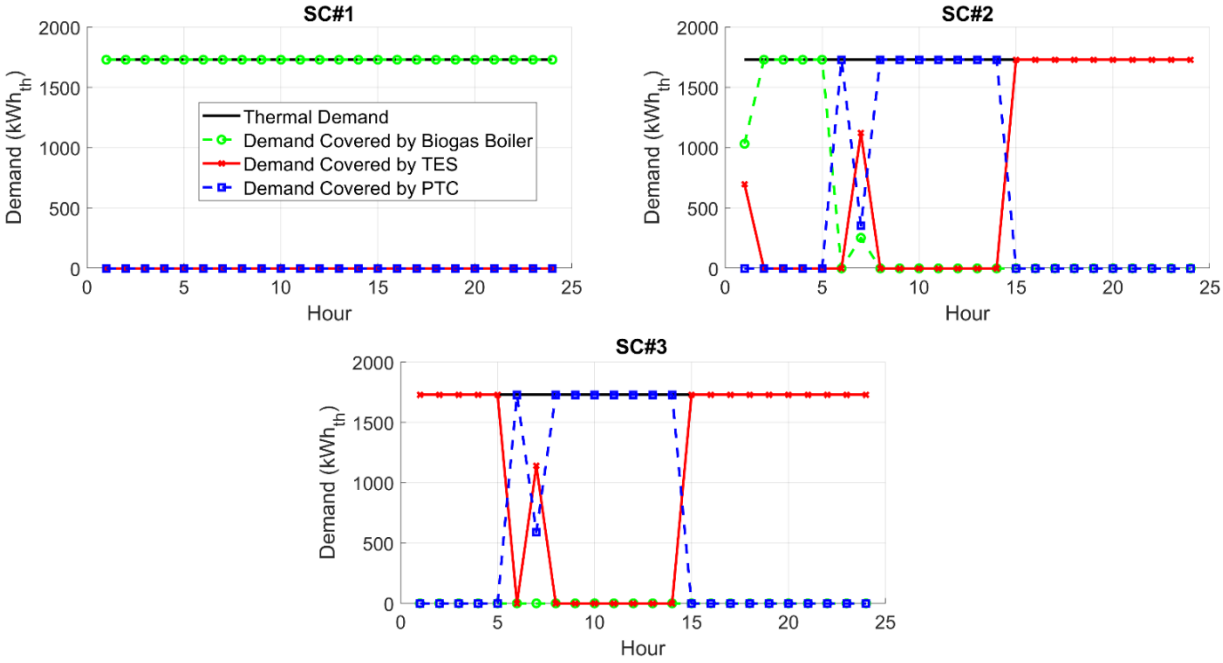

503

504 **Figure 8:** Thermal demand covered by biogas boiler, PTC and TES for Dec 1st.

In the context of the plant's electrical energy demand, Figure 9 (a) illustrates the portion of the monthly electrical demand covered by the grid for each scenario. As observed from the figure, Scenario 1 demonstrates a high dependency on grid-supplied electricity, with an average monthly value of 800 MWh throughout the year. With the integration of PV and PTC systems, along with TES, scenarios 2 and 3 witness a significant reduction in their reliance on the grid, especially during the summer season. Notably, SC# 3 exhibits the lowest grid dependency, courtesy of its larger PTC and PV system sizes. This transition towards reduced grid dependence is further highlighted in Figure 9 (b), where the PV systems in scenarios 2 and 3 contribute significantly to covering the electrical demand, with an average contribution of 2,000 MWh and 2,500 MWh, respectively.

Considering the electrical energy surplus generated through the introduction of PV and PTC systems, the plant is poised to produce an excess of electrical energy, as depicted in Figure 9 (c). This surplus energy is expected to reach 3000 MWh for SC#3 where it can be stored as a user energy credit for the plant at the grid network. However, it's worth noting that due to JEPCO company's policy in Jordan, the plant is currently unable to sell this excess energy, leaving it unutilized. Nevertheless, this situation paves the way for potential future modifications within the plant to leverage this surplus energy for various other applications.

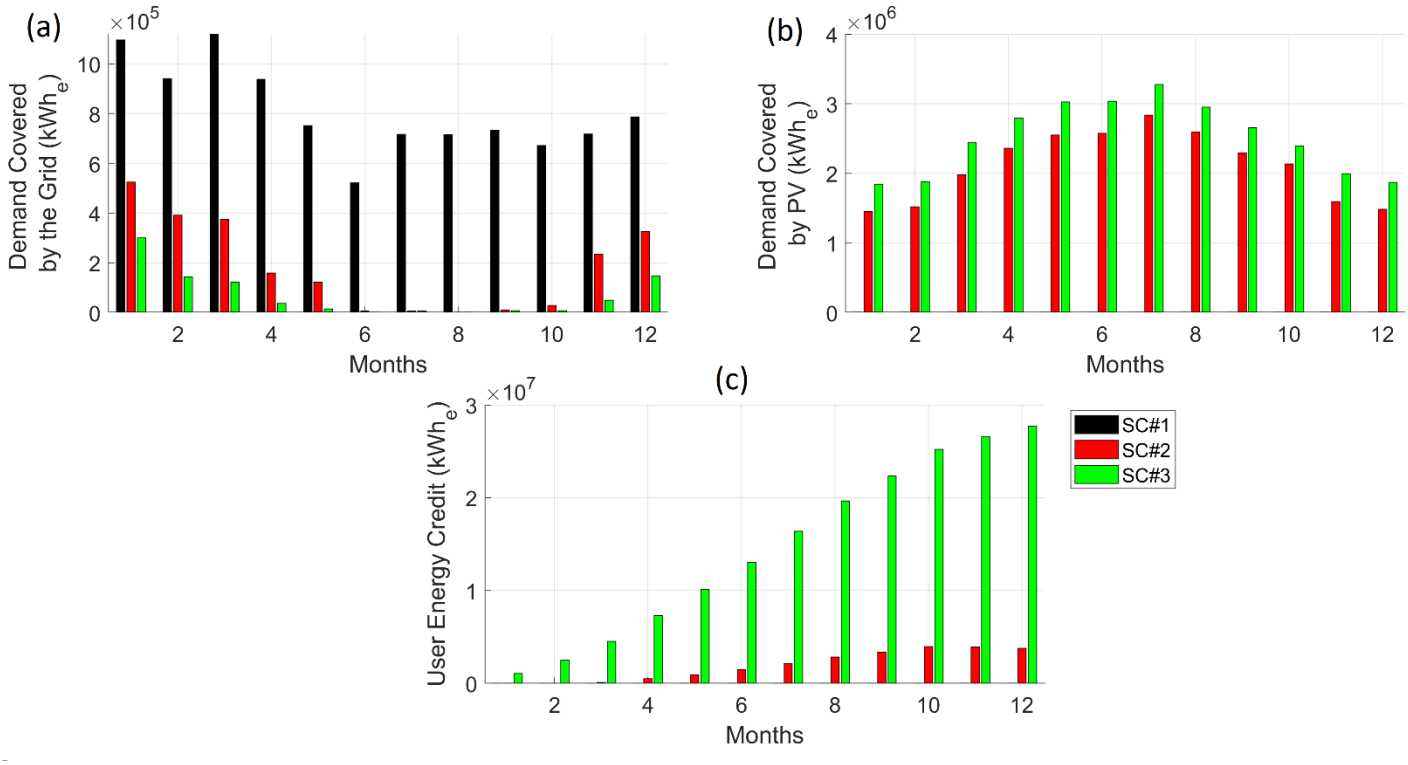

522 **Figure 9**: Demands covered by the grid and PV system in addition to the user energy credit.

523 In Table 5, a comprehensive comparison among the three scenarios is presented, focusing on capital
524 installation costs, annual operating and maintenance expenses, and the yearly electricity bill. In SC#1,
525 the annual electricity bill is notably the highest, exceeding 2 million USD. However, in SC#2 and
526 SC#3, this amount is substantially reduced to around 86,000 USD and nearly zero USD, receptively
527 even though there is still dependency on the grid. This reduction in the electricity bill is attributed to
528 both reduction in the energy drawn from the grid and also the PV excess energy credits which is used
529 to offset the utility bill.

530 It is essential to acknowledge that both scenarios 2 and 3 entail initial capital costs for the installation
531 of PV, PTC, and TES systems. Additionally, these scenarios incur ongoing operating and maintenance
532 expenses for the integrated systems. By examining the reduction in the annual electricity bill
533 achievable through the implementation of scenarios 2 and 3, it becomes evident that the cost savings

not only offset the capital and operational expenditures but also render both scenarios economically viable for the plant. This financial feasibility is further substantiated by considering the NPV values for the three scenarios, with scenarios 2 and 3 exhibiting positive NPV values. The positive NPV signifies that both scenarios yield tangible economic benefits, reinforcing their attractiveness and viability for the plant.

Table 5: Capital, operational costs and annual electricity bill for the three scenarios

Cost ($)	SC#1	SC#2	SC#3
Capital cost of PV	-	15,020,116.19	28,493,217.29
Capital cost of PTC	-	1,487,163.30	2,476,362.41
Capital cost of Battery	-	-	-
Capital cost of TES	-	254,565.44	696,806.96
Annual O&M PV	-	97,069.31	184,140.84
Annual O&M PTC	-	140,298.42	233,619.10
Annual Electricity bill	2,184,091.05	86,347.18	-

It should be noted that the power purchase (PP) tariff, no information was available on it from the operator and hence it was assumed to be half the utility tariff in Jordan, affects the economics of the system and hence it is important to assess the effect of it on the economics of the system. Figure 10 (a) and 9 (b) illustrate the impact of the PP tariff on the LCOE and NPV values. In Figure 10 (a), the LCOE value remains constant for SC#1 since almost no electricity from biogas/hydro is sold to grid.

However, for both scenarios 2 and 3, the LCOE value exhibits a decreasing trend. The power purchase tariff, or the price at which a facility can sell its excess electrical energy to the grid, has a notable impact on the LCOE. A higher power purchase tariff reduces the LCOE by increasing the revenue generated from selling excess electricity. This makes renewable energy systems more economically attractive and can lead to greater adoption of clean and sustainable energy sources. Furthermore, an increase in the power purchase tariff leads to higher NPV values for both SC#2 and SC#3. An increase in the power purchase tariff leads to higher NPV values because it generates more revenue, resulting in positive cash flows that, when discounted to present value, increase the net value or profit expected from the applied scenario. The subtle distinctions between SC#2 and SC#3 concerning LCOE and NPV values are mainly driven by variations in their respective capital costs. Additionally, SC#3 allocates a greater proportion of biogas for thermal demands rather than electrical needs, thereby contributing to a relatively higher LCOE value and a decreased NPV value in comparison to SC#2.

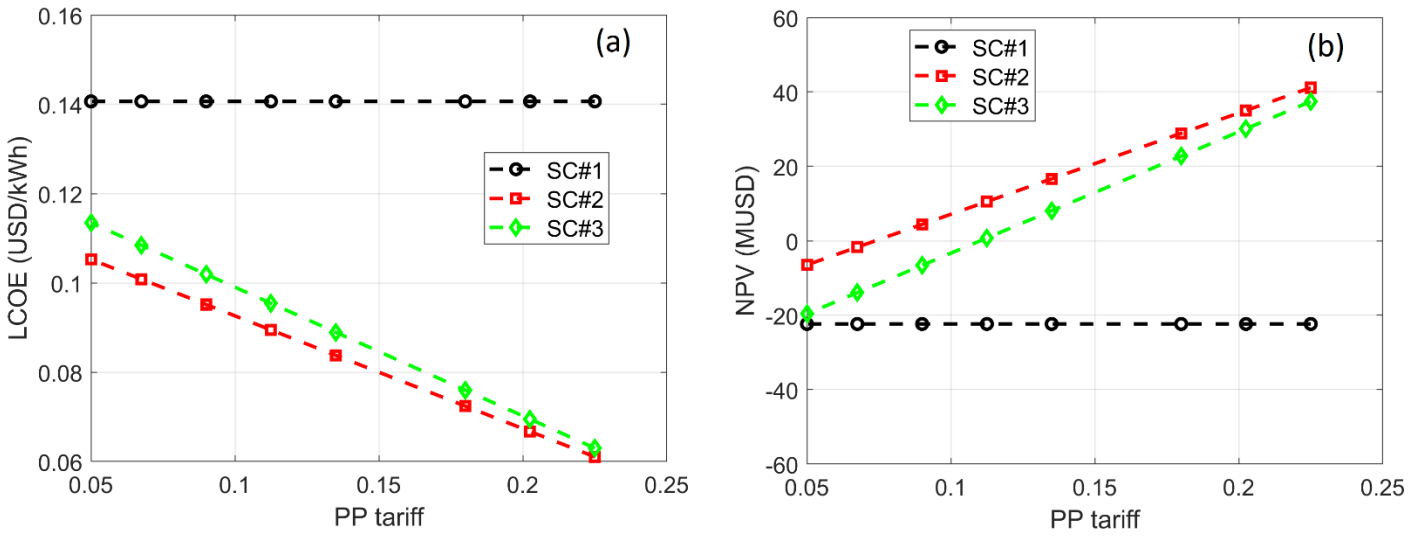

Figure 10: Power purchase tariff vs (a) LCOE and (b) NPV value for the three main scenarios.

4. Conclusions

The current study underscores the crucial role of integrating renewable energy sources, particularly solar energy, into WWTPs to enhance energy and environmental sustainability. Focused on As Samra WWTP in Jordan, the investigation focused on two primary solar energy systems, each offering distinct advantages. The first system, combining parabolic trough collectors (PTCs) with thermal energy storage (TES), aimed to reduce reliance on biogas boilers for digesters' heat supply, thereby increasing biogas availability for electricity generation. The second system involved a PV panels that will directly fulfil a portion of the plant's electricity demands.

The study explored two optimization scenarios: one prioritizing the NPV and the LCOE, and the other minimizing the LCOH. Key outcomes included a remarkable reduction in grid reliance to just 1-3%, a significant decrease in biogas contribution to electricity generation from 88% to around 65%, and substantial cuts in thermal demand from biogas boilers. Notably, Scenario #2 achieved the most favourable LCOE value of 0.0895 USD/kWh with an NPV of 10.54 million USD, while Scenario #3 attained an LCOH value of 0.0432 USD/kWh_{th}. Overall, both scenarios substantially reduced annual electricity expenditure and enabled surplus energy generation and storage for future utilization or direct marketing.

In addition to the findings, future research suggests the integration of multiple renewable energy sources alongside solar energy, such as wind and geothermal energy sources, which could further bolster WWTPs' energy autonomy and resilience. Also, exploring the utilization of waste heat and mass in WWTPs could contribute to more sustainable WWTPs. Moreover, renewable energy can be utilized in some post-treatment process of water like water desalination and disinfection, which will expand the role of WWTPs. In addition to that, WWTPs can a play a significant role in producing many useful products like green Hydrogen and Ammonia, allowing for more economic sustainability

for these facilities. By embracing these forward-looking perspectives and fostering interdisciplinary collaborations, the transition towards sustainable wastewater treatment practices can be accelerated, thus contributing significantly to climate change mitigation and environmental stewardship.

References

2030 Solar Cost Targets. (n.d.). Energy.Gov. Retrieved October 24, 2023, from https://www.energy.gov/eere/solar/articles/2030-solar-cost-targets

Aghabalaei, V., Nayeb, H., Mardani, S., Tabeshnia, M., & Baghdadi, M. (2023). Minimizing greenhouse gases emissions and energy consumption from wastewater treatment plants via rational design and engineering strategies: A case study in Mashhad, Iran. *Energy Reports*, *9*, 2310–2320. https://doi.org/10.1016/j.egyr.2023.01.017

Al-Ghussain, L., Ahmad, A. D., Abubaker, A. M., Abujubbeh, M., Almalaq, A., & Mohamed, M. A. (2021). A demand-supply matching-based approach for mapping renewable resources towards 100% renewable grids in 2050. *Ieee Access*, *9*, 58634–58651.

Al-Ghussain, L., Ahmad, A. D., Abubaker, A. M., & Hassan, M. A. (2022). Techno-economic feasibility of thermal storage systems for the transition to 100% renewable grids. *Renewable Energy*, *189*, 800–812.

Al-Ghussain, L., Ahmed, H., & Haneef, F. (2018). Optimization of hybrid PV-wind system: Case study Al-Tafilah cement factory, Jordan. *Sustainable Energy Technologies and Assessments*, *30*, 24–36. https://doi.org/10.1016/j.seta.2018.08.008

Ali, S. M. H., Lenzen, M., Sack, F., & Yousefzadeh, M. (2020). Electricity generation and demand flexibility in wastewater treatment plants: Benefits for 100% renewable electricity grids. *Applied Energy*, *268*, 114960. https://doi.org/10.1016/j.apenergy.2020.114960

607 Bey, M., Hamidat, A., & Nacer, T. (2021). Eco-energetic feasibility study of using grid-connected
608 photovoltaic system in wastewater treatment plant. *Energy*, *216*, 119217.
609 https://doi.org/10.1016/j.energy.2020.119217
610 Boretti, A., & Castelletto, S. (2021). Techno-economic performances of future concentrating solar
611 power plants in Australia. *Humanities and Social Sciences Communications*, *8*(1), 1–10.
612 Brachi, P., Di Fraia, S., Massarotti, N., & Vanoli, L. (2022). Combined heat and power production
613 based on sewage sludge gasification: An energy-efficient solution for wastewater treatment
614 plants. *Energy Conversion and Management: X*, *13*, 100171.
615 https://doi.org/10.1016/j.ecmx.2021.100171
616 Buller, L. S., Sganzerla, W. G., Berni, M. D., Brignoli, S. C., & Forster-Carneiro, T. (2022). Design
617 and techno-economic analysis of a hybrid system for energy supply in a wastewater treatment
618 plant: A decentralized energy strategy. *Journal of Environmental Management*, *305*, 114389.
619 https://doi.org/10.1016/j.jenvman.2021.114389
620 CanadianSolar. (2021). *HiKu5 Mono PERC*.
621 Capodaglio, A. G., & Olsson, G. (2020). Energy Issues in Sustainable Urban Wastewater
622 Management: Use, Demand Reduction and Recovery in the Urban Water Cycle. *Sustainability*,
623 *12*(1), Article 1. https://doi.org/10.3390/su12010266
624 Chen, S., & Chen, B. (2013). Net energy production and emissions mitigation of domestic wastewater
625 treatment system: A comparison of different biogas–sludge use alternatives. *Bioresource*
626 *Technology*, *144*, 296–303. https://doi.org/10.1016/j.biortech.2013.06.128
627 Cole, W. J., & Frazier, A. (2019). *Cost projections for utility-scale battery storage*. National
628 Renewable Energy Lab.(NREL), Golden, CO (United States).

Duffie, J. A., & Beckman, W. A. (2006). Solar engineering of thermal processes. In *Solar Engineering of Thermal Processes: Fourth Edition* (3rd ed). Wiley. https://doi.org/10.1002/9781118671603

Đurđević, D., Blecich, P., & Jurić, Ž. (2019). Energy Recovery from Sewage Sludge: The Case Study of Croatia. *Energies*, *12*(10), Article 10. https://doi.org/10.3390/en12101927

Dutta, V., Sonu, Sudhaik, A., Kumar, R., Raizada, P., Ahamad, T., Alshehri, S. M., Thakur, S., Van Le, Q., Kaya, S., Hu, C., Nguyen, V.-H., & Singh, P. (2024). Emergence of S-scheme-derived Ag decorated CuBi2O4/CNTs/(BiO)2CO3 photocatalyst with enhanced visible light photocatalytic performance. *Journal of the Taiwan Institute of Chemical Engineers*, *156*, 105319. https://doi.org/10.1016/j.jtice.2023.105319

Epp, B. (2018). Molten salt storage 33 times cheaper than lithium-ion batteries. *Solar Therm.(12)*.

EU Science Hub, Non-interactive service. (2023). https://ec.europa.eu/jrc/en/PVGIS/docs/noninteractive

Gandiglio, M., Lanzini, A., Soto, A., Leone, P., & Santarelli, M. (2017). Enhancing the Energy Efficiency of Wastewater Treatment Plants through Co-digestion and Fuel Cell Systems. *Frontiers in Environmental Science*, *5*. https://www.frontiersin.org/articles/10.3389/fenvs.2017.00070

Garcia, C., Pérez-Sánchez, M., Ramos, H. M., López-Jiménez, P. A., & Sánchez-Romero, F.-J. (2024). New strategies in wastewater treatment plants to evaluate the achievement of sustainable development goals: A case study. *Urban Water Journal*, *0*(0), 1–12. https://doi.org/10.1080/1573062X.2024.2323962

Guo, J., Zhang, W., Zhang, J., Xie, L., Zeng, X., Zhong, J., Zhao, O., Yang, K., Li, Z., Zou, R., Bai, Z., Wang, Q., & Zhang, C. (2024). Carbon reduction measures-based life cycle assessment of

the photovoltaic-supported sewage treatment system. *Sustainable Cities and Society*, *101*, 105074. https://doi.org/10.1016/j.scs.2023.105074

Huld, T., Müller, R., & Gambardella, A. (2012). A new solar radiation database for estimating PV performance in Europe and Africa. *Solar Energy*, *86*(6), 1803–1815.

Jaber, J., Al-Sarkhi, A., Akash, B., & Mohsen, M. (2004). Medium-range planning economics of future electrical-power generation options. *Energy Policy*, *32*(3), 357–366.

Jacob, R., Short, M., Belusko, M., & Bruno, F. (2020). Maximising renewable gas export opportunities at wastewater treatment plants through the integration of alternate energy generation and storage options. *Science of The Total Environment*, *742*, 140580. https://doi.org/10.1016/j.scitotenv.2020.140580

Khan, A. A. P., Sonu, Sudhaik, A., Raizada, P., Khan, A., Rub, M. A., Azum, N., Alotaibi, M. M., Singh, P., & Asiri, A. M. (2023). AgI coupled SiO2@CuFe2O4 novel photocatalytic nano-material for photo-degradation of organic dyes. *Catalysis Communications*, *179*, 106685. https://doi.org/10.1016/j.catcom.2023.106685

Kiselev, A., Magaril, E., & Karaeva, A. (2024). Environmental and economic efficiency assessment of biogas energy projects in terms of greenhouse gas emissions. *Energy, Ecology and Environment*, *9*(1), 68–83. https://doi.org/10.1007/s40974-023-00305-5

Maktabifard, M., Zaborowska, E., & Makinia, J. (2018). Achieving energy neutrality in wastewater treatment plants through energy savings and enhancing renewable energy production. *Reviews in Environmental Science and Bio/Technology*, *17*(4), 655–689. https://doi.org/10.1007/s11157-018-9478-x

Malhotra, M., Sudhaik, A., Sonu, Raizada, P., Ahamad, T., Nguyen, V.-H., Van Le, Q., Selvasembian, R., Mishra, A. K., & Singh, P. (2023). An overview on cellulose-supported photocatalytic

materials for the efficient removal of toxic dyes. *Industrial Crops and Products*, *202*, 117000. https://doi.org/10.1016/j.indcrop.2023.117000

Mannina, G., Mofatto, P. M. B., Cosenza, A., Di Trapani, D., Gulhan, H., Mineo, A., & Makinia, J. (2024). The effect of aeration mode (intermittent vs. Continuous) on nutrient removal and greenhouse gas emissions in the wastewater treatment plant of Corleone (Italy). *Science of The Total Environment*, 171420. https://doi.org/10.1016/j.scitotenv.2024.171420

Masłoń, A., Czarnota, J., Szaja, A., Szulżyk-Cieplak, J., & Łagód, G. (2020). The Enhancement of Energy Efficiency in a Wastewater Treatment Plant through Sustainable Biogas Use: Case Study from Poland. *Energies*, *13*(22), Article 22. https://doi.org/10.3390/en13226056

Mattioli, A., Gatti, G. B., Mattuzzi, G. P., Cecchi, F., & Bolzonella, D. (2017). Co-digestion of the organic fraction of municipal solid waste and sludge improves the energy balance of wastewater treatment plants: Rovereto case study. *Renewable Energy*, *113*, 980–988. https://doi.org/10.1016/j.renene.2017.06.079

Maziotis, A., Sala-Garrido, R., Mocholi-Arce, M., & Molinos-Senante, M. (2023). A comprehensive assessment of energy efficiency of wastewater treatment plants: An efficiency analysis tree approach. *Science of The Total Environment*, *885*, 163539.

Myszograj, S., Bocheński, D., Mąkowski, M., & Płuciennik-Koropczuk, E. (2021). Biogas, Solar and Geothermal Energy—The Way to a Net-Zero Energy Wastewater Treatment Plant—A Case Study. *Energies*, *14*(21), Article 21. https://doi.org/10.3390/en14216898

Myszograj, S., & Qteishat, O. (2011). Operate of As-Samra wastewater treatment plant in Jordan and suitability for water reuse. *Inżynieria i Ochrona Środowiska*, *14*, 29–40.

Nourin, F. N., Abbas, A. I., Qandil, M. D., & Amano, R. S. (2020). Analytical Study to Use the Excess Digester Gas of Wastewater Treatment Plants. *Journal of Energy Resources Technology*, *143*(012104). https://doi.org/10.1115/1.4047603

Obaideen, K., Shehata, N., Sayed, E. T., Abdelkareem, M. A., Mahmoud, M. S., & Olabi, A. G. (2022). The role of wastewater treatment in achieving sustainable development goals (SDGs) and sustainability guideline. *Energy Nexus*, *7*, 100112. https://doi.org/10.1016/j.nexus.2022.100112

Parrado, C., Marzo, A., Fuentealba, E., & Fernández, A. (2016). 2050 LCOE improvement using new molten salts for thermal energy storage in CSP plants. *Renewable and Sustainable Energy Reviews*, *57*, 505–514.

Patial, S., Sonu, Thakur, S., Van Le, Q., Ahamad, T., Singh, P., Nguyen, V.-H., Khan, A. A. P., Hussain, C. M., & Raizada, P. (2023). Facile synthesis of Co, Fe-bimetallic MIL-88A/microcrystalline cellulose composites for efficient adsorptive and photo-Fenton degradation of RhB dye. *Journal of the Taiwan Institute of Chemical Engineers*, *153*, 105189. https://doi.org/10.1016/j.jtice.2023.105189

Patial, S., Sudhaik, A., Sonu, Thakur, S., Van Le, Q., Ahamad, T., Singh, P., Huang, C.-W., Nguyen, V.-H., & Raizada, P. (2024). Synergistic interface engineering in n-p-n type heterojunction Co3O4/MIL/Mn-STO with dual S-scheme multi-charge migration to enhance visible-light photocatalytic degradation of antibiotics. *Environmental Research*, *240*, 117481. https://doi.org/10.1016/j.envres.2023.117481

Płuciennik-Koropczuk, E., Myszograj, S., & Mąkowski, M. (2022). Reducing CO2 Emissions from Wastewater Treatment Plants by Utilising Renewable Energy Sources—Case Study. *Energies*, *15*(22), Article 22. https://doi.org/10.3390/en15228446

719 Sadecka, Z., Bochenski, D., Myszograj, S., & Suchowska-Kisielewicz, M. (2013). Green Energy from
720 Biogas in a Polish-German Sewage Treatment Plant. *Energy Sources, Part A: Recovery,*
721 *Utilization, and Environmental Effects*, *35*(13), 1249–1255.
722 https://doi.org/10.1080/15567036.2012.751469
723 SAFT, A. (2013). *Range of Ready-to-Install Containerised Energy Storage for Renewable Energies*
724 *and Grid Management*.
725 Santos, I. F. S. dos, Barros, R. M., & Tiago Filho, G. L. (2016). Electricity generation from biogas of
726 anaerobic wastewater treatment plants in Brazil: An assessment of feasibility and potential.
727 *Journal of Cleaner Production*, *126*, 504–514. https://doi.org/10.1016/j.jclepro.2016.03.072
728 Schuetze, B., & Hussein, H. (2023). The geopolitical economy of an undermined energy transition:
729 The case of Jordan. *Energy Policy*, *180*, 113655. https://doi.org/10.1016/j.enpol.2023.113655
730 Tavakoli, N., Khoshkenar, P., & Pourfayaz, F. (2024). A combined approach-based techno-economic-
731 environmental multi-optimization of a hydrogen generation system through waste biomass air-
732 steam gasification. *Renewable Energy*, 120259. https://doi.org/10.1016/j.renene.2024.120259
733 Tomczyk, P., Mastalerek, K., Wiatkowski, M., Kuriqi, A., & Jurasz, J. (2023). Assessment of a Francis
734 Micro Hydro Turbine Performance Installed in a Wastewater Treatment Plant. *Energies*,
735 *16*(20), 7214.
736 Xi, J., Gong, H., Zhang, Y., Dai, X., & Chen, L. (2021). The evaluation of GHG emissions from
737 Shanghai municipal wastewater treatment plants based on IPCC and operational data
738 integrated methods (ODIM). *Science of The Total Environment*, *797*, 148967.
739 https://doi.org/10.1016/j.scitotenv.2021.148967
740 Zahmatkesh, S., Amesho, K. T. T., Sillanpaa, M., & Wang, C. (2022). Integration of renewable energy
741 in wastewater treatment during COVID-19 pandemic: Challenges, opportunities, and

progressive research trends. *Cleaner Chemical Engineering*, *3*, 100036. https://doi.org/10.1016/j.clce.2022.100036

Zakariazadeh, A., Ahshan, R., Al Abri, R., & Al-Abri, M. (2024). Renewable energy integration in sustainable water systems: A review. *Cleaner Engineering and Technology*, *18*, 100722. https://doi.org/10.1016/j.clet.2024.100722

Zhang, X., Hao, T., Zhang, T., Hu, Y., Lu, R., Li, D., Pan, Y., Li, Y.-Y., & Kong, Z. (2024). Towards energy conservation and carbon reduction for wastewater treatment processes: A review of carbon-neutral anaerobic biotechnologies. *Journal of Water Process Engineering*, *59*, 105026. https://doi.org/10.1016/j.jwpe.2024.105026

Zhu, W., Duan, C., & Chen, B. (2024). Energy efficiency assessment of wastewater treatment plants in China based on multiregional input–output analysis and data envelopment analysis. *Applied Energy*, *356*, 122462. https://doi.org/10.1016/j.apenergy.2023.122462